HiSST: 2nd International Conference on
High-Speed Vehicle Science Technology
11-15 September 2022, Bruges, Belgium

Molecular Beam Studies of Carbon and Silicon Carbide Ablation by Atomic Oxygen and Nitrogen

Vanessa J. Murray[1], David Z. Chen[1], Chenbiao Xu[2], Pedro Recio[3], Adriana Carocciolo[3], Chloe Miossec[3], Piergiorgio Casavecchia[3], Savio Poovathingal,[4] Timothy K. Minton[2]

Abstract

Molecular beam-surface scattering experiments have been used to obtain fundamental data on gas-surface interactions that are central to the ablation of carbon and silicon carbide (SiC) during hypersonic flight through air. Specifically, the reactions of O and N atoms on high-temperature carbon surfaces have been studied, and the reactions of O atoms and passive-to-active oxidation phenomena have been studied on SiC. The reactive scattering dynamics of O on various carbon surfaces suggest that the oxidation mechanisms on all sp^2 types of carbon are similar but that surface morphology influences the relative importance of the individual mechanisms. In addition to reacting with carbon to produce CO_2 (minor product) and CO (major product), oxygen atoms may recombine on the surface to produce O_2 with an efficiency that is somewhat lower than that to produce CO. Nitrogen atoms may recombine on the surface to produce N_2 or react to produce CN. The recombination efficiency of N atoms is generally more than an order of magnitude higher than the reaction efficiency to produce CN. Even a small percentage of N atoms in the presence of O atoms can increase the reactivity of O atoms on a carbon surface by more than 50%. Impingement of O atoms on SiC forms an oxide layer at lower temperatures, which decomposes through the release of SiO and probably Si atoms at approximately 1670 K. With lower O-atom flux, a graphene-like layer persists on the surface at higher temperatures, but with a higher O-atom flux, the surface ablates to produce CO and SiO products. By determining individual chemical mechanisms at a molecular level, as well as their reaction probabilities, ablation models may be developed that are not tied to a specific test environment.

Keywords: *Molecular beam, atomic oxygen, carbon oxidation, carbon nitridation, silicon carbide oxidation*

Nomenclature

FiberForm – carbon fiber preform
TOF – time of flight
HOPG – highly oriented pyrolytic graphite
θ_i – angle of incidence
θ_f – scattering, or final, angle
TEA – transversely excited atmospheric
RF – radio frequency
$N(t)$ – number density distribution as a function of time

[1] *Dept. of Chemistry and Biochemistry, Montana State University, Bozeman, Montana 59717, United States,* vanessa.j.murray@gmail.com, davidzuyuchen@gmail.com
[2] *Smead Dept. of Aerospace Engineering Sciences, University of Colorado, Boulder, Colorado 80303, United States,* tminton@colorado.edu
[3] *Dipartimento di Chimica, Biologia e Biotecnologie, Universita' degli Studi di Perugia, 06123 Perugia, ITALY,* piero@dyn.unipg.it
[4] *Department of Mechanical Engineering, University of Kentucky, Lexington, KY 40506, USA;* saviopoovathingal@uky.edu

$P(E_T)$ – probability distribution as a function of translational energy
$P(V)$ – probability distribution as a function of velocity
IS – impulsive scattering
TD – thermal desorption
m/z – mass-to-charge ratio
XPS – X-ray photoelectron spectroscopy

1. Introduction

Understanding the oxidation and nitridation mechanisms of carbon and ceramic materials is key to the reliable design of heat shields for hypersonic flight through air. We have been using molecular beam-surface scattering experiments to gain an understanding of the high temperature oxidation and nitridation of model materials [1-8]. We have conducted extensive investigations of O and/or N atoms with three types of carbon at high temperatures, (1) highly oriented pyrolytic graphite (HOPG) [2], (2) vitreous carbon [1,5,6], and (3) carbon fiber preform (FiberForm) [7]. The molecular beam-surface scattering results for carbon have been used in the development of an air-carbon ablation finite-rate model [8]. New work has recently been conducted to gain an initial understanding of the detailed oxidation mechanisms of a model, single-crystal silicon carbide (SiC) surface by atomic oxygen. This paper provides a review of the molecular beam-surface scattering studies that have been performed on carbon, as well as a presentation of new results on the oxidation of SiC.

2. Experimental Methods

The experiments have been performed with the use of two molecular beam sources coupled to a molecular beam apparatus with a rotatable mass spectrometer detector (see Fig. 1). A pulsed laser-detonation molecular beam source (Fig. 1a) was used to produce hyperthermal beams of O and O_2, N and N_2, or a combination nitrogen and oxygen. A pulse of O_2, N_2, or mixture of O_2 and N_2 gas at high pressure (~40 bars) is injected into the throat of a conical nozzle, and a 7 J pulse^{-1} CO_2 TEA laser is fired. The light is focused into the throat of the nozzle and induces a breakdown, creating a high-temperature plasma. The resulting shock wave dissociates and accelerates the gas, and the emerging gas pulse contains atomic and molecular species with a nominal velocity of ~8 km s^{-1}. The atomic fraction can be 60% to more than 90%, depending on source operating conditions. The beam pulse has a broad velocity distribution, so we use a synchronized chopper wheel to select a narrow range of velocities from the overall beam pulse. A typical example of the beam composition and the translational

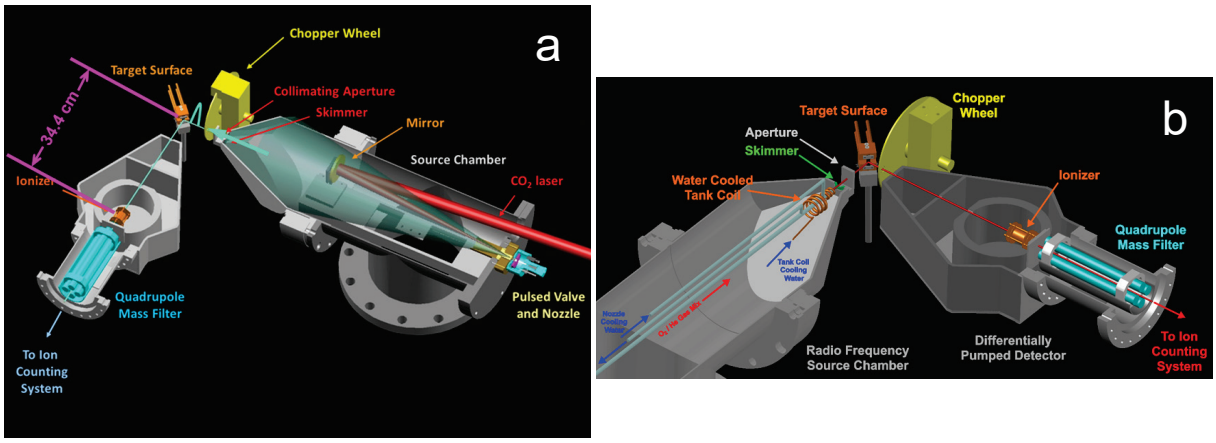

Fig 1. (a) Molecular beam-surface scattering set-up with pulsed laser-detonation beam source. The velocity-selecting chopper wheel, heated sample, and rotatable mass spectrometer detector are shown. Scattered products are monitored as a function of their arrival time at the ionizer of the detector time after the beam pulse strikes the surface. (b) Molecular beam-surface scattering set-up with the high-pressure RF discharge source. The continuous beam from this source strikes a heated surface, and the scattered products are modulated with a chopper wheel; the resultant pulses of products are detected as a function of their arrival time in the rotatable mass spectrometer.

energy distributions of the O and O components is shown in Fig. 2a. The velocity-selected pulse strikes a surface, and the products that scatter are detected with a rotatable mass spectrometer detector. Samples are often heated by passing current through a sample that is mounted between two water-cooled copper electrodes. Vitreous carbon and FiberForm samples were heated by passing current directly through them; HOPG was heated radiatively by placing it on top of a heated vitreous carbon sample. The second source used was a radio frequency (RF) discharge source (Fig. 1b), which produced continuous beams of partially dissociated gas with nominal velocities of ~2 km s^{-1}. For the oxygen beam, an 85 mbar mixture of 5% O_2 in He was discharged with an RF power of 300 W and then expanded through a 0.48 mm diameter water-cooled quartz nozzle. The nitrogen beam was produced with a 95 mbar mixture of 2.5% N_2 in He and discharged with an RF power of 250 W and expanded through the same nozzle. An example of the velocity distributions of the O and O_2 components of an oxygen beam are shown in Fig. 2b. The beam was collimated with apertures before striking a hot carbon surface. Products that scattered from the surface were detected with the rotatable mass spectrometer detector. A chopper wheel was used to modulate the products that came off the surface, so that their velocities could be determined using the time-of-flight method. In experiments with both sources, our primary data are number density distributions as a function of flight time, *N(t)*, from the sample surface (Fig. 1a) or chopper wheel (Fig. 1b) to the ionizer of the mass spectrometer detector, which are commonly referred to as time-of-flight (TOF) distributions. These TOF distributions may be collected at a variety of final (or scattering angles, θ_f) for a given incident angle, θ_i. The TOF distributions may be transformed into velocity distributions, *P(V)*, or translational energy distributions, $P(E_T)$, which are both proportional to flux [9].

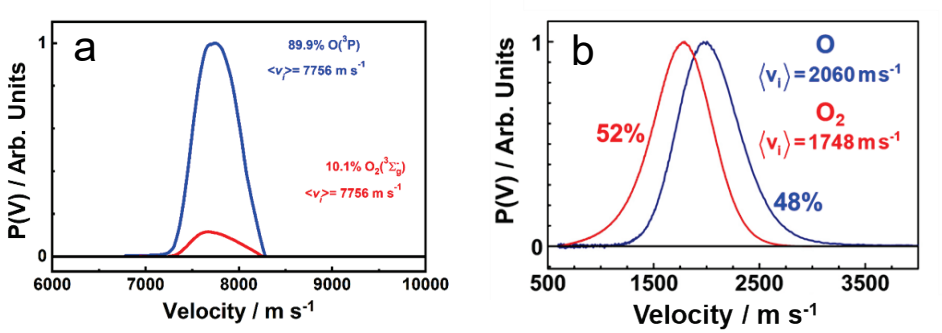

Fig 2. (a) Velocity distributions of components of the molecular beam produced from the laser-detonation source. (b) Velocity distributions of components of the molecular beam produced from the RF discharge source. In both panels, the average velocities and mole fractions of the species are shown.

3. Results and Discussion

Gas-surface scattering may be described in terms of two limiting cases of interactions that are either thermal or non-thermal [9,10]. Atoms or molecules that scatter non-thermally through impulsive scattering (IS) or by Eley-Rideal reactions have relatively high exit velocities (short flight times) and lobular angular directions that peak roughly in the specular direction. Molecules that desorb thermally after trapping momentarily or reacting through a Langmuir-Hinshelwood reaction typically have a near-Maxwell-Boltzmann distribution of velocities (long flight times) and a cosine angular distribution of scattered flux. This is often referred to as thermal desorption (TD), or "diffuse scattering". The data thus can distinguish between products that scatter on a timescale too short for thermal equilibrium to be attained and products that desorb in thermal equilibrium with the surface. The reactive scattering dynamics of 7.8 km s^{-1} atomic oxygen on all three carbon surfaces are similar, yet the details of the dynamics differ. As may be seen in the TOF distributions in Fig. 3, inelastically scattered O and O_2 and reactively scattered CO and CO_2 were observed. For O and O_2, both non-thermal and thermal processes were seen. It was evident that the thermal scattering of O atoms grew with increasing surface temperature. O_2 scattered mainly by impulsive scattering at all surface temperatures, whereas CO and CO_2 appeared to desorb thermally. The signal from CO rose and then fell (or levelled off) with increasing surface temperature. And the CO_2 signal decreased with surface temperature and there was no CO_2 produced at higher temperatures above roughly 1200 K. The similar trends but different details of the

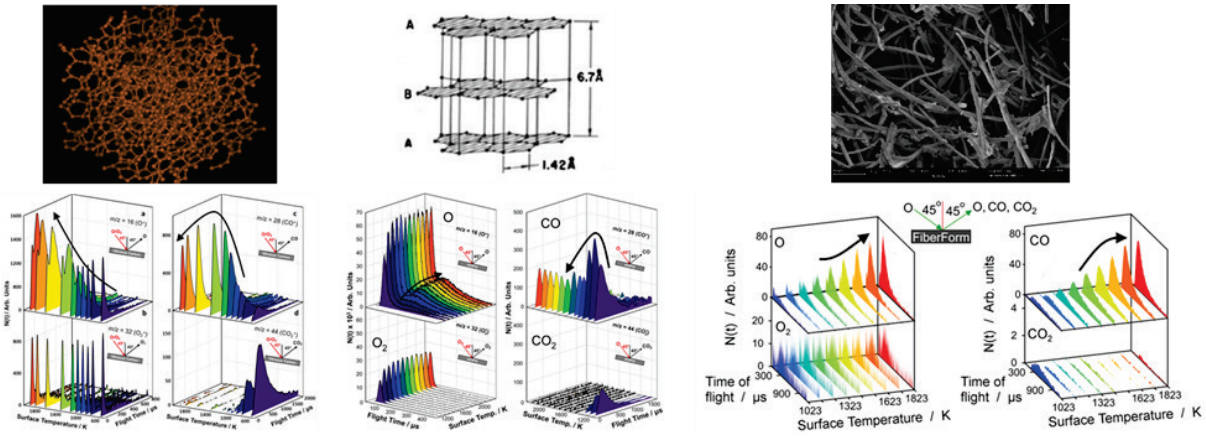

Fig 3. *Above:* Representations of the three types of carbon studied, vitreous carbon, HOPG, and carbon fiber preform. *Below:* Time-of-flight distributions of O, O_2, CO, and CO_2 products scattering from three types of carbon as a function of surface temperature, with θ_i = 46° and θ_f = 45°, for experiments that used the pulsed laser-detonation source of O atoms. The O_2 signal is almost entirely from direct scattering of O_2 that is in the incident beam, not from O-atom recombination.

results from the three types of carbon suggest that the morphology of the carbon material influences the relative importance of the mechanisms. Furthermore, the data indicate that the reaction mechanisms occur in thermal equilibrium with the surface and that the surface oxygen coverage is high except at the highest temperatures.

Lower-velocity, higher-flux, and continuous O-atom beams were used to investigate the scattering dynamics of atomic oxygen on a vitreous carbon surface, and reaction efficiencies of the four scattering pathways were determined and are shown in Fig. 4. The results agree with the general conclusions of the experiments that were conducted with the very different hyperthermal O-atom beam (summarized above), which was pulsed and had 4x higher velocity. But this new experiment with a continuous beam has allowed reaction efficiencies to be determined, and we were able to observe and quantify the recombination of O atoms to produce O_2. As observed in the experiments with the hyperthermal pulsed beam, the CO was the dominant reactive product, and its efficiency decreased at higher temperatures. Although the O-O recombination efficiency is not insignificant, the efficiency for this process is significantly less than reaction to form CO. A thorough analysis of all the molecular beam scattering data on the high-temperature oxidation of carbon by O atoms has led to the general picture that is depicted in Fig. 5. Incoming O atoms increase surface coverage and lower the barriers to CO and CO_2

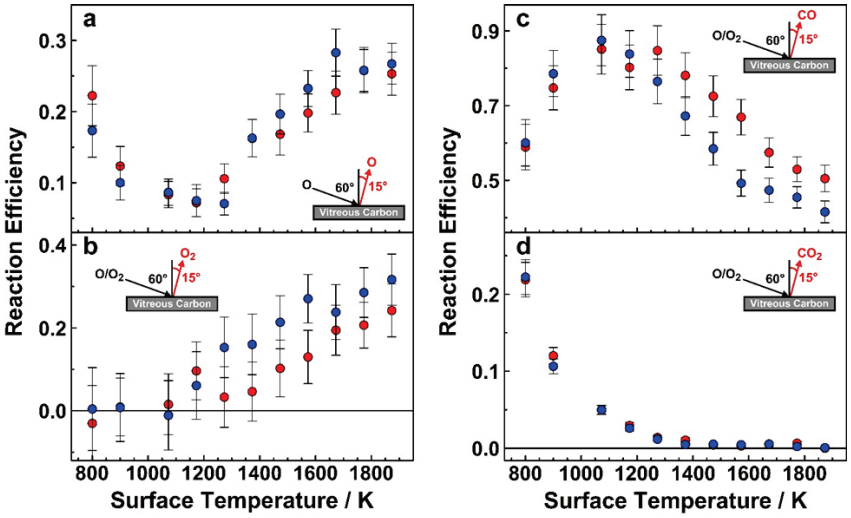

Fig 4. Reaction efficiencies of O, O_2, CO, CO_2 as a function of surface temperature following bombardment of the vitreous carbon surface by O atoms from the RF discharge source. The red symbols correspond to data collected when the surface temperature was increased, whereas the blue symbols correspond to data collected when the surface temperature was decreased. Error bars indicate 95% confidence limit.

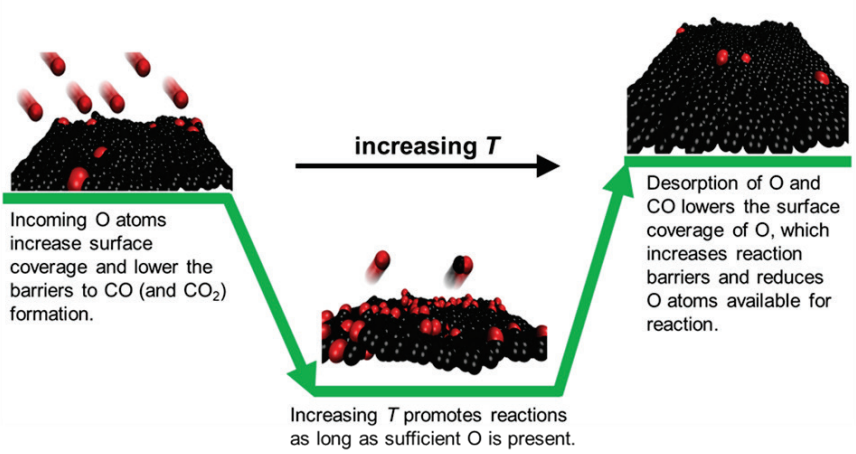

Fig 5. General picture of carbon oxidation by O atoms at high temperatures.

formation. Increasing surface temperature promotes reactions as long as sufficient O is present. At high temperatures, desorption of O and CO lowers the surface coverage of O, which increases reaction barriers and reduces the number of surface O atoms that are available for reaction, thus lowering the reactivity of carbon with O atoms. A higher flux of O atoms on the surface can maintain the surface coverage of oxygen and allow high reactivity even at higher temperatures. There are both prompt and slow processes that lead to the production of CO reaction products, and the rates of all these processes must be considered in a finite rate model. When the temperature is raised, the CO signal is higher than when the temperature is lowered. A hysteresis in the temperature dependence of the O and CO efficiencies is observed, where the reaction efficiency as the surface temperature is increased is different than it is when the surface temperature is decreased. This is because surface O-atom coverage is needed for the CO to be formed, and when the surface becomes hotter, the O atoms desorb and the coverage decreases. When the surface is heated from a relatively low temperature, the oxygen coverage is high, and the reactivity is high, but when the temperature is lowered from a higher temperature, the surface oxygen coverage starts out lower, and the reactivity is lower. When the reactivity is higher, more O leaves the surface in the form of CO, so the O-atom flux from the surface is lower, and when the reactivity is lower, less O leaves the surface in the form of CO, so the O-atom flux is higher. Thus, there is an anticorrelation in the hysteresis of the O and CO signals (refer to Fig. 4).

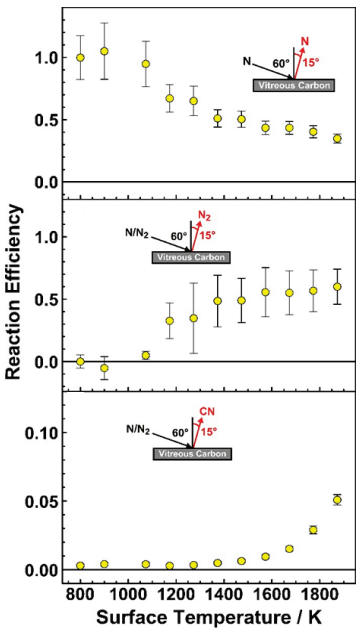

Fig 6. Reaction efficiencies of N, N_2, and CN as a function of surface temperature, when O atoms from the RF discharge source bombard a vitreous carbon surface.

Experiments with N-atom interactions on vitreous carbon using the RF discharge source (see Fig. 6) have revealed that N atoms may recombine on the surface to produce N_2 or react to produce CN. The probability of recombination of N atoms may be an order of magnitude higher than the reaction probability to produce CN. The rate of production of CN rises dramatically with temperature and has allowed us to determine an activation energy of ~172 kJ mol^{-1} for the process(es) to produce CN. The N-atom reaction probability to produce CN on a pristine vitreous carbon surface is always less than 5% the reaction probability of the O-atom reactivity to produce CO on a pristine surface, regardless of surface temperature (see Fig. 7).

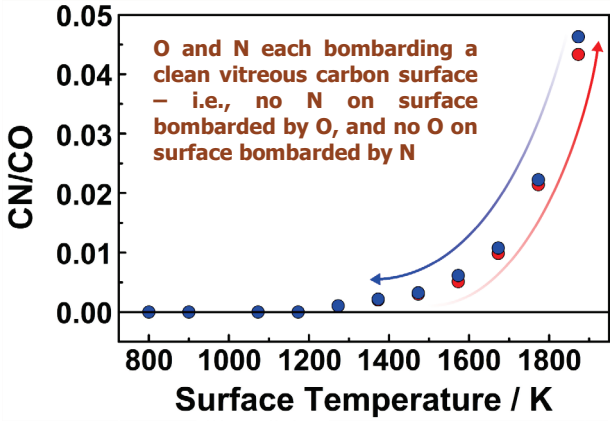

Fig 7. Ratio of CN to CO flux as a function of surface temperature for θ_i = 60° and θ_f = 15°. The red symbols correspond to CO fluxes when the surface temperature was increased, whereas the blue symbols correspond to CO fluxes when the surface temperature was decreased; the CN flux was the same at a given surface temperature regardless of whether the sample was being heated or cooled.

In an effort to determine the effect of N atoms on the O-atom reactivity with carbon to produce CO, we carried out a rather elaborate set of experiments with hyperthermal beams containing O and/or N atoms [6]. A summary of the results is shown in Fig. 8. The CO flux produced from bombardment of a vitreous carbon surface by a beam containing N and O atoms was compared with the CO flux produced from bombardment by beams containing either N or O atoms. The presence of small mole fractions of N atoms of 0.02-0.08 enhanced the reactivity of O atoms by a factor of 1.4-1.6 in the range of surface

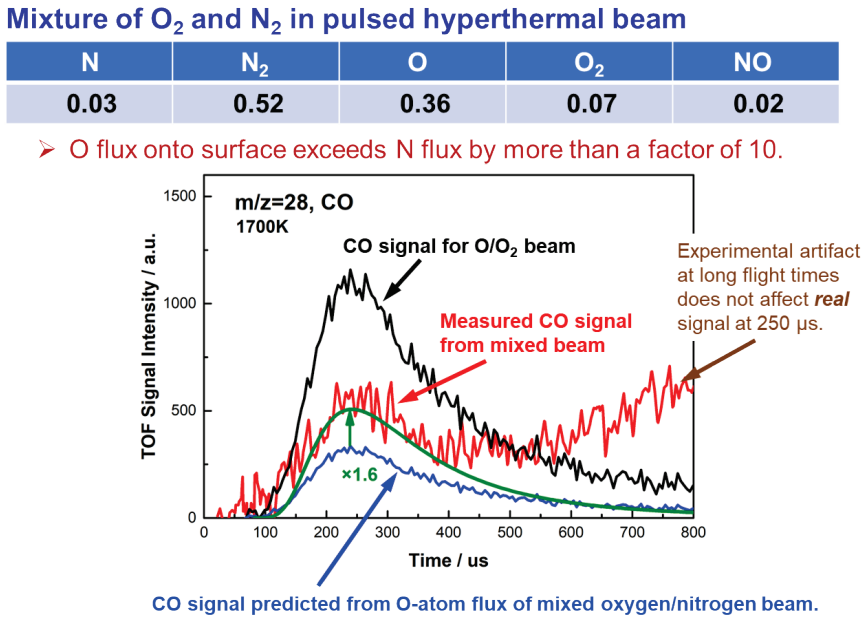

Fig 8. Summary of results on the effect of N atoms on the O-atom reactivity with vitreous carbon, with a surface temperature of 1700 K. The mole fractions of the hyperthermal beam that produced a 1.6x enhancement in reactivity over a hyperthermal oxygen beam (with the same flux of O atoms in both cases) is shown at the top of the figure.

temperatures from 1100 to 1700 K. A detailed explanation of the observed results requires more study, but it appears that N atoms can act as a catalyst to increase the reactivity of O with carbon and that a relatively low flux of N atoms may be sufficient to saturate the catalytic effect.

In new studies, we have investigated the mechanism of the temperature range of the passive-to-active oxidation transition in the interaction between atomic and molecular oxygen and the surface of 6H-SiC and 6H-SiC oxidized with a roughly 5 nm-thick oxide layer. This study used the hyperthermal beam, consisting of O and O_2 in a 97:3 mole ratio, and additional experiments were conducted with the RF discharge source, whose characteristics are shown in Fig. 2b.

Before studies of O-atom interactions with SiC samples commenced, we first oxidized them by exposing them to a high fluence of O atoms (~1×10^{20} O atoms cm^{-2}) with the hyperthermal O-atom beam in the source chamber [11,12]. This created an oxide layer on the surface, which was verified by XPS analysis to be predominantly SiO_2. Then we placed oxidized samples in a heated sample mount in the vacuum chamber (base pressure ~ 10^{-7} Torr) in front of our mass spectrometer for further experimentation (see Fig. 1a). An initial study was conducted by heating the sample with no bombardment from the molecular beam and monitoring the mass spectrum of products that came off the surface as the sample was heated. As seen in Fig. 9, a sudden spike was observed in the signal at a mass-to-charge ratio (*m/z*) of 44 signal at about 1670 K, and then this signal went away as the temperature was increased further. This signal was identified as $^{28}Si^{16}O$ based on the small signals from the minor isotopes at $^{29}Si^{16}O$ and $^{30}Si^{16}O$. Thus, when the sample is heated without O-atom exposure, the oxide layer is removed as SiO gas at a temperature of ~1670 K. This temperature is identified as the passive-to-active oxidation transition temperature under the high vacuum conditions of our chamber.

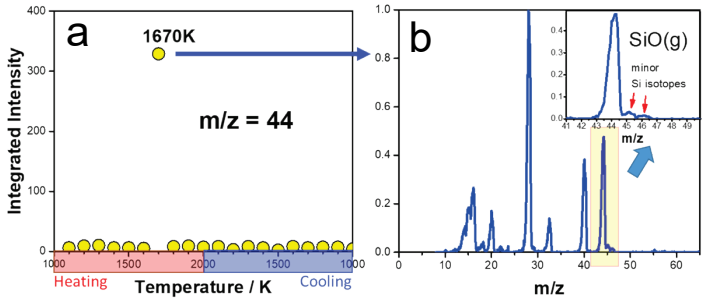

Fig 9. (a) Integrated intensity of the signal observed at m/z = 44 as a pre-oxidized SiC sample was heated from 1000 K to 2000 K and then cooled back to 1000 K. (b) Mass spectrum of gaseous products from SiC at 1670 K including background gases in the mass spectrometer Note that the signal from background CO_2 (*m/z* = 44) is small compared to the SiO signal.

In a second study, we placed a sample that had been pre-oxidized in the same manner as described above in the heated sample mount and conducted a molecular beam-surface scattering experiment. The experimental set-up was the same as that shown on the right side of Fig. 1a. For this experiment, a pulsed hyperthermal beam containing 93% O and 7% O_2, with an average velocity of 7770 m s^{-1}, was used without velocity selection with a chopper wheel. While this beam was impinging on the surface at an incident angle of θ_i = 45°, TOF distributions were collected at *m/z* = 16, 32, 28, and 44 as a function of surface temperature at a final angle of θ_f = 10°. A low final angle of 10° was chosen because products that desorbed from the surface in thermal equilibrium were expected to give the highest signal along the surface normal. During data collection, the sample was heated from 1123 K to 1973 K in (mostly) 100 K increments and then the temperature was reduced in (mostly) 100 K increments until the sample temperature reached its initial value. The results are summarized in Fig. 10. Below the passive/active transition temperature, incident O atoms scatter directly through impulsive scattering (IS) – there is no evidence for thermal accommodation of O on the SiO_2 surface. When the sample temperature rises above the passive/active transition, there is an abrupt change in the scattering dynamics of O, as the O that exits the surface desorbs in thermal equilibrium with the surface. The thermal desorption of O atoms is very similar to the results that we have observed previously in analogous molecular beam-surface scattering experiments on carbon [1,2]. O_2, which is present in the incident beam, appeared to scatter impulsively at lower temperatures, and then the signal became very weak and made the scattering dynamics very difficult to discern at temperatures above the

passive/active transition. The reduction in the O_2 signal at θ_f = 10° is likely the result of a change in the angular distribution of the O_2 products, which shifted to larger angles because the surface became covered with a smooth graphitic layer (see below). At lower temperatures and near the transition temperature, signals detected at *m/z* = 28 and 44 are negligible. When the sample approaches the passive/active transition temperature, it appears that there is a sudden increase in the evolution of products that are detected at *m/z* = 28 and 44. We believe that the *m/z* = 28 signal may arise from Si atoms and CO molecules that are released, perhaps through a reaction, proposed by Raider et al. [13,14], that occurs at the oxide-substrate interface: $2SiC(s) + SiO_2(s) \rightarrow 3Si(g,l,s) + 2CO(g)$. The *m/z* = 44 signal almost certainly arises from SiO. Both signals drop dramatically as the temperature is incremented further. Assuming the assignment of the signals is correct, then it seems that, as the passive/active transition is approached, the oxide layer breaks down quickly and products thermally desorb from the surface at relatively high fluxes; then these signals decline quickly as the temperature increases further. The lack of reactive signals (*m/z* = 28 and 44) at temperatures well above the passive/active transition temperature indicates surface passivation. When the surface temperature is reduced, reactive signals at *m/z* = 28 and 44 appear, and the O signal has the dynamical character that is representative of thermal desorption, which is qualitatively different than the O signals that were observed originally from the oxidized SiC surface.

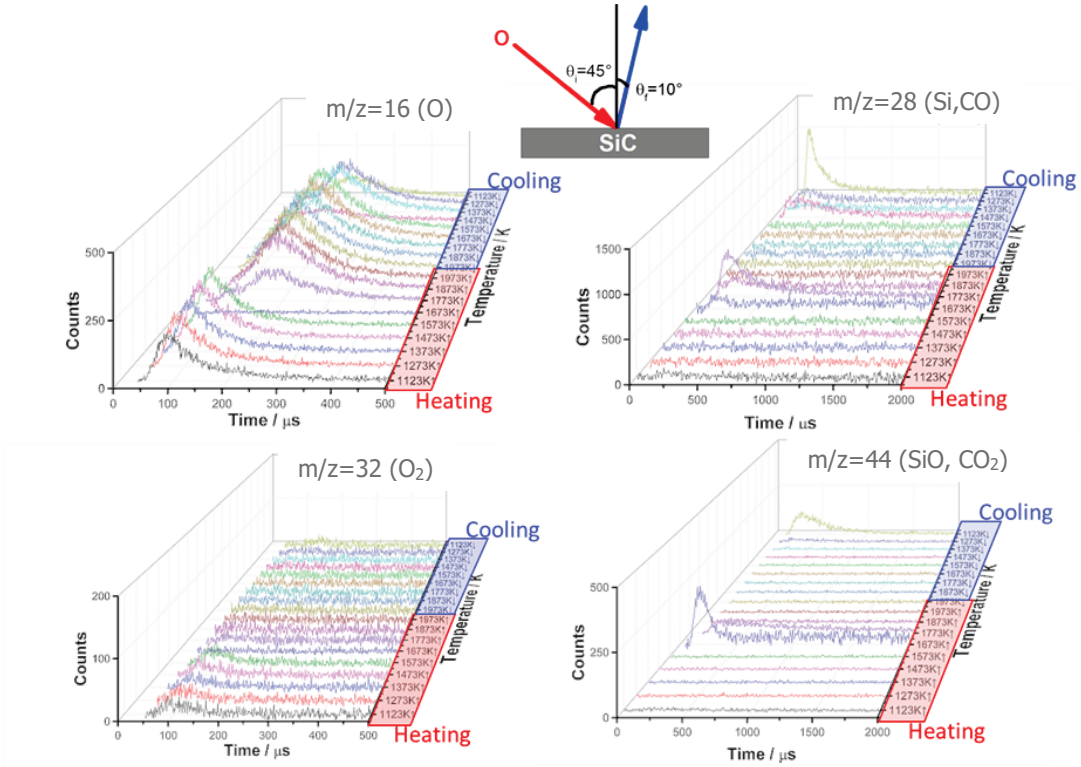

Fig 10. Time-of-flight distributions of *m/z* = 16, 32, 28, and 44 products scattering from oxidized SiC as a function of surface temperature, using the pulsed hyperthermal source of atomic oxygen. Incident and final angles are shown at the top of the figure. A pre-oxidized sample was exposed to the beam and the sample was first heated and then cooled as the data were collected.

XPS analysis of the surfaces on SiC that resulted from different treatments was performed and compared to XPS analysis of a pristine 6H-SiC surface (see Fig. 11). These results are consistent with the formation of a graphitic layer on the surface after the oxidized SiC sample was heated to a temperature above the passive/active transition. Finally, the presence of a graphitic layer was also confirmed by a Raman scattering analysis of the surface that had been heated to 1973 K (not shown).

The results from the hyperthermal O-atom beam studies thus suggest a picture where SiO and Si are released from an oxidized SiC surface in a passive-to-active transition at about 1670 K and leave a graphitic carbon layer that is not etched away by the relatively low flux of O atoms from the beam. If the flux of O atoms were higher, as in a real hypersonic flow (or a plasma torch facility), then the graphitic layer would presumably react more quickly to form CO, and it would not be passivating. With the removal of the passivating graphitic layer on an SiC surface that is above the passive/active

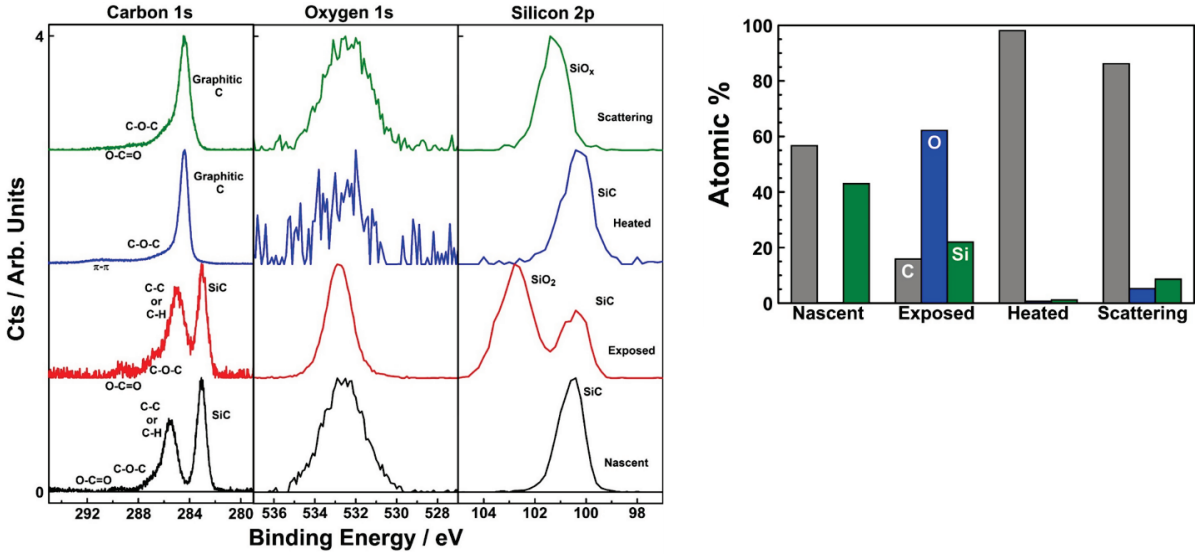

Fig 11. XPS results from a pristine SiC surface (Nascent), an SiC surface that was oxidized in the hyperthermal O/O_2 beam, 40 cm from the source, at room temperature (Exposed), an SiC surface that had been first oxidized at room temperature and then heated to 1973 K in vacuum (Heated), and an SiC surface that had been first oxidized at room temperature and then heated to a temperature of 1973 K and then cooled to 1123 K, all during bombardment by the O/O_2 beam at a distance of 99 cm from the source (Scattering). The "Scattering" sample was used during the collection of the data shown in Fig. 10.

transition temperature, incident O atoms could then react with SiC to form volatile SiO and CO. This active oxidation regime would result in etching of the SiC, and it could possibly result in a temperature jump [15] because the reactions are exothermic and would release heat to the surface. Given our data on the formation of a passivating graphitic layer, one might speculate that the delay in the temperature jump after the passive/active transition temperature has been reached [15] might be the result of a passivating graphitic layer that needs to be removed before the full suite of high-temperature oxidation reactions can take place, although this idea is yet to be proven.

In order to break through the passivating graphitic layer and probe the volatile oxidation products of SiC during active oxidation, we conducted a molecular beam-surface scattering experiment with the continuous beam from the RF discharge O-atom source (Fig. 1b), which had 2-3 orders of magnitude higher O-atom flux than the pulsed hyperthermal beam used for the experiments described above. The flux of O atoms onto the sample surface was estimated to be 4×10^{16} atoms cm^{-2} s^{-1}. The continuous beam was directed at a heated 6H-SiC surface, and the products that scattered from the surface were detected with a rotatable mass spectrometer after being modulated with the chopper wheel in front of the detector. The TOF distributions for the four *m/z* ratios where signal was observed with continuous O-atom bombardment of the 6H-SiC surface are shown in Figure 12. The signal at *m/z* = 16 comes from the thermal desorption of O atoms that underwent no net reaction on the surface. These unreacted O atoms presumably desorbed thermally because the surface became extremely rough during exposure to the O-atom beam, allowing for multiple bounces on the surface, which drove O atoms toward thermal equilibrium. The TOF distributions remain unchanged with increasing surface temperature until 1773 K, when the signal suddenly drops, probably because the reactivity of the incident O atoms increases abruptly. The signal at *m/z* = 32 arises mostly from non-reactive scattering of O_2 molecules that are in the incident beam. These molecules apparently come into thermal equilibrium with the surface before desorbing. It is also possible that some fraction of the O_2 signal comes from O-atom recombination on the surface, although this process was not investigated. The O_2 TOF distributions also remain essentially unchanged with surface temperature until a temperature of 1773 K is reached, at which point the O_2 signal suddenly drops. Either O_2 can react with the SiC surface at this high temperature or the changes in the surface at this temperature reduce the likelihood of O-atom recombination. There is very little signal detected at *m/z* = 28 at lower surface temperatures, and the signal at this *m/z* ratio increases dramatically when the surface temperature reaches 1773 K. This observation is consistent with a process where the surface is covered with a passivating oxide layer at lower temperatures, resulting from bombardment by oxygen atoms, and then the oxide layer decomposes at a high temperature and

allows the O atoms to react with the SiC to produce CO. This explanation assumes that a passive-to-active transition occurs at a temperature that is slightly lower than 1773 K. Given that the experiments with the pre-oxidized surface described above exhibited a clear passive/active transition at ~1670 K, the somewhat higher temperature of the passive/active transition during exposure to the continuous O-atom beam suggests that the higher O-atom flux of this beam delays the onset of the transition. The signal at m/z = 44 also dramatically increases above the passive/active transition to a temperature of ~1773 K. This signal is the result of O-atom reactions to form SiO. Thus, it appears that, at high temperatures where a passivating oxide has decomposed, active oxidation of SiC by atomic oxygen leads to continuous production of CO and SiO, which etches the surface.

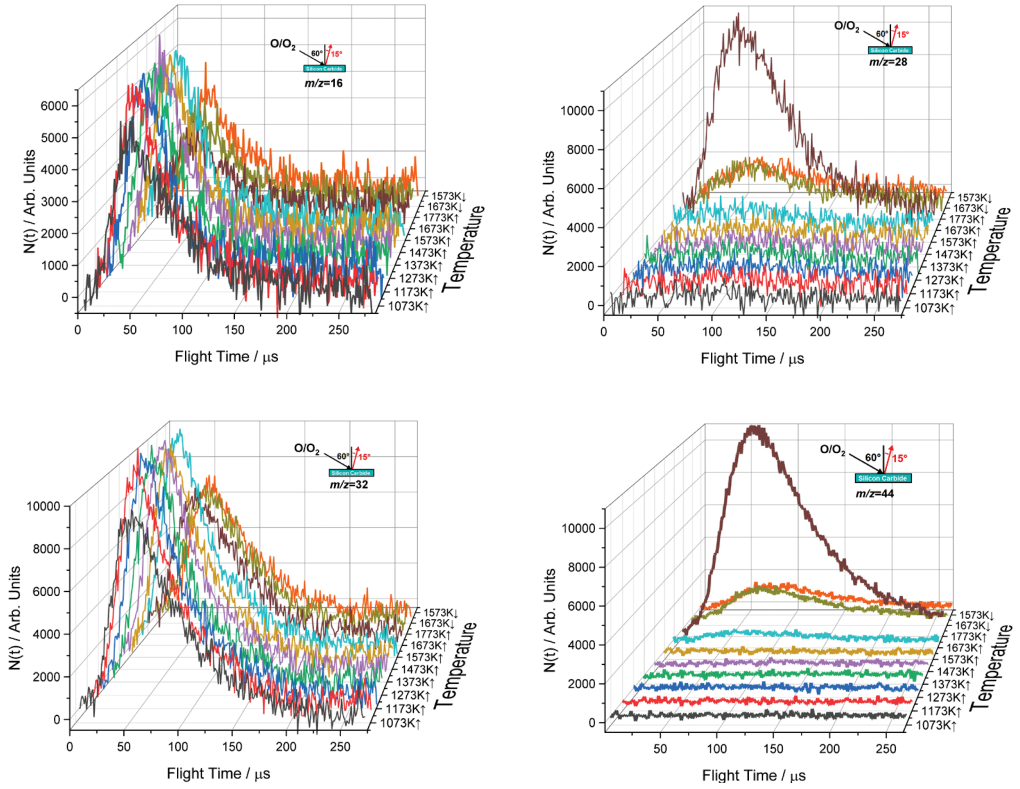

Fig. 12. Time-of-flight distributions of scattered products collected at m/z = 16, 32, 28, and 44 at a final angle of θ_f = 15°, following bombardment of a 6H-SiC surface by the continuous beam from the RF discharge source, with an incident angle of θ_i = 60°. The sample was brought to 1073 K and then heated in 100 K steps to 1773 K and then cooled back to 1573 K in 100 K steps, after which data collection stopped and the sample was cooled to room temperature and removed from the chamber.

4. Conclusion

To gain a better understanding the gas-surface reactions on heat shield materials during hypersonic flight through air, we have used molecular beam-surface scattering experiments to study reactions of O and N atoms on high-temperature carbon and SiC surfaces. The experiments were performed with both pulsed and continuous molecular beams of O or N atoms and, in some cases, mixed beams containing both O and N atoms.

Our studies of the oxidation of three forms of carbon – vitreous carbon, HOPG, and Fiberform – strongly suggest that the differences observed in the interactions of oxygen atoms with these various forms of carbon are a result of the qualitatively different morphology of the three sp^2 carbon materials and not significant differences in the chemical mechanisms. The efficiencies of the gas-surface interactions, both reactive and non-reactive, were quantified as a function of surface temperature. The volatile products of oxygen reactions with carbon were CO (major) and CO_2 (minor). Oxygen atoms may also react with each other (recombine) on the surface to produce O_2 with an efficiency that is somewhat

lower than that to produce CO. The production rate of CO increases and then decreases as the surface temperature is increased, because surface-adsorbed oxygen, which helps to promote the reaction of oxygen with carbon at lower temperatures, desorbs at higher temperatures. Nitrogen atoms may react to produce CN, but the reactivity of N with a pristine vitreous carbon surface to produce CN is <5% the reactivity of O atoms with the same surface to produce CO. Under N-atom bombardment, the recombination efficiency of N atoms is generally more than an order of magnitude higher than the reaction efficiency to produce CN. Even a small percentage of N atoms in the presence of O atoms can increase the reactivity of O atoms on a carbon surface by more than 50%. The data from these studies have been used in the formulation of an air-carbon ablation model [8].

The oxidation of SiC was investigated below and above the passive-to-active transition temperature. With the hyperthermal O-atom beam, it was observed that raising the surface temperature above 1670 K results in transient signals at *m/z* = 28 and 44, followed by their subsequent suppression as the surface became graphitized. With the use of a higher-flux supersonic O-atom beam, continuous production of products with these *m/z* ratios was observed above the passive-to-active transition temperature. The corresponding products were determined to be CO and SiO from the isotopic signature of silicon. In a study of an oxidized SiC surface, conducted without atomic-oxygen bombardment, as the temperature passed through the passive-to-active transition point, key gas phase products were Si atoms and SiO molecules. Above the passive-to-active transition temperature, the oxide layer completely disappeared, leaving a graphite layer on the SiC surface. The results of all the studies suggest that, during O-atom bombardment of an SiC surface at high temperatures, there is a competition between the formation graphitic carbon and reactive production of volatile CO and SiO that depends on the flux of atomic oxygen onto the surface. Although more work would need to be done to understand the details of the passive-active transition, we speculate that the limited reactivity of graphite to oxygen at high temperatures may temporarily protect the SiC bulk from fully active oxidation until the graphitic layer has been removed. The abrupt removal by atomic oxygen of a partially passivating graphitic layer at temperatures above the passive/active transition would expose the highly reactive SiC bulk to rapid exothermic oxidation to CO and SiO, possibly resulting in a temperature jump.

Acknowledgments

This work was supported by the US Air Force Office of Scientific Research (Grant Numbers FA9550-10-1-0563 and FA9550-17-1-0057), and by NASA (Grant Numbers NNX15AD77G and 80NSSC18M006). V.J.M. is grateful for support from the Department of Defense (DoD) through the US National Defense Science & Engineering Graduate Fellowship (NDSEG) Program. The views and conclusions contained herein are those of the authors and should not be interpreted as necessarily representing the official policies or endorsements, either expressed or implied, of the AFOSR or the U.S. Government.

References

1. Murray, V. J.; Marshall, B. C.; Woodburn, P. J.; Minton, T. K. Inelastic and Reactive Scattering Dynamics of Hyperthermal O and O_2 on Hot Vitreous Carbon Surfaces. *J. Phys. Chem. C* **2015**, *119*, 14780-14796.
2. Murray, V. J.; Smoll, Jr., E. J.; Minton, T. K. Dynamics of Graphite Oxidation at High Temperatures. *J. Phys. Chem. C* **2018**, *122*, 6602-6617.
3. Poovathingal, S. J.; Schwartzentruber, T. E.; Murray, V. J.; Minton, T. K.; Candler, G. V. Finite-Rate Oxidation Model for Carbon Surfaces from Molecular Beam Experiments. *AIAA J.* **2017**, *55*, 1644-1658.
4. Swaminathan-Gopalan, K.; Borner, A.; Murray, V. J.; Poovathingal, S. J.; Minton, T. K.; Mansour, N. N.; Stephani, K. A. Development and Validation of a Finite-Rate Model for Carbon Oxidation by Atomic Oxygen. *Carbon* **2018**, *137*, 313-332.
5. Murray, V. J.; Recio, P.; Caracciolo, A.; Miossec, C.; Balucani, N.; Casavecchia, P.; Minton, T. K. Oxidation and Nitridation of Vitreous Carbon at High Temperatures. *Carbon* **2020**, 167, 388-402.

6. Xu, C.; Minton, T. K. Effect of N Atoms on O-Atom Reactivity with Carbon. *J. Spacecr. Rockets* **2021**, *58*, 906-909.
7. Poovathingal, S. J.; Qian, M.; Murray, V. J.; Minton, T. K. Reactive and Inelastic Scattering Dynamics of Hyperthermal O and O_2 from a Carbon Fiber Network. *Carbon* **2021**, *183*, 277-290.
8. Prata, K. S.; Schwartzentruber, T. E.; Minton, T. K. Air-Carbon Ablation Model for Hypersonic Flight from Molecular Beam Data. *AIAA J.* **2022**, *60*, 627-640.
9. Minton, T. K.; Giapis, K. P.; Moore, T. Inelastic Scattering Dynamics of Hyperthermal Fluorine Atoms on a Fluorinated Silicon Surface. *J. Phys. Chem. A* **1997**, *101*, 6549-6555.
10. Kleyn, A. W. Molecular Beams and Chemical Dynamics at Surfaces. *Chem. Soc. Rev.* **2003**, *32*, 87−95.
11. Wright, J. S.; Jones, A.; Farmer, B.; Rodman, D. L.; Minton, T. K. POSS-Enhanced Colorless Organic/Inorganic Nanocomposite (CORIN®) for Atomic Oxygen Resistance in Low Earth Orbit. *CEAS Space J.* **2021**, *13*, 399-413.
12. Minton, T. K.; Schwartzentruber, T. E.; Xu, C. On the Utility of Coated POSS-Polyimides for Vehicles in Very Low Earth Orbit. *ACS Appl. Mater. Interfaces* **2021**, *13*, 51673-51684.
13. Raider, S. I.; Herd, S. R.; Walkup, R. E., SiO_2 film decomposition reaction initiated by carbon impurities located at a Si-SiO_2 interface. *Appl. Phys. Lett.* **1991**, *59*, 2424-2426.
14. Raider, S. I., Carbon impurities at a Si-SiO_2 interface. *Microelect. Eng.* **1993**, *22*, 29-34.
15. Panerai, F.; Helber, B.; Chazot, O.; Balat-Pichelin, M. Surface temperature jump beyond active oxidation of carbon/silicon carbide composites in extreme aerothermal conditions. *Carbon* **2014**, *71*, 102-119.